



SCHOOL of
GRADUATE STUDIES
EAST TENNESSEE STATE UNIVERSITY

East Tennessee State University
Digital Commons @ East
Tennessee State University

Electronic Theses and Dissertations

Student Works

5-2018

Eyring Activation Energy Analysis of Acetic Anhydride Hydrolysis in Acetonitrile Cosolvent Systems

Nathan Mitchell

East Tennessee State University

Follow this and additional works at: <https://dc.etsu.edu/etd>

 Part of the [Analytical Chemistry Commons](#)

Recommended Citation

Mitchell, Nathan, "Eyring Activation Energy Analysis of Acetic Anhydride Hydrolysis in Acetonitrile Cosolvent Systems" (2018). *Electronic Theses and Dissertations*. Paper 3430. <https://dc.etsu.edu/etd/3430>

This Thesis - Open Access is brought to you for free and open access by the Student Works at Digital Commons @ East Tennessee State University. It has been accepted for inclusion in Electronic Theses and Dissertations by an authorized administrator of Digital Commons @ East Tennessee State University. For more information, please contact digilib@etsu.edu.

Eyring Activation Energy Analysis of Acetic Anhydride Hydrolysis in Acetonitrile Cosolvent
Systems

A thesis

presented to

the faculty of the Department of Chemistry

East Tennessee State University

In partial fulfillment

of the requirements for the degree

Master of Science in Chemistry

by

Nathan Mitchell

May 2018

Dr. Dane Scott, Chair

Dr. Greg Bishop

Dr. Marina Roginskaya

Keywords: Thermodynamic Analysis, Hydrolysis, Linear Solvent Energy Relationships,
Cosolvent Systems, Acetonitrile

ABSTRACT

Eyring Activation Energy Analysis of Acetic Anhydride Hydrolysis in Acetonitrile Cosolvent Systems

by

Nathan Mitchell

Acetic anhydride hydrolysis in water is considered a standard reaction for investigating activation energy parameters using cosolvents. Hydrolysis in water/acetonitrile cosolvent is monitored by measuring pH vs. time at temperatures from 15.0 to 40.0 °C and mole fraction of water from 1 to 0.750. This work utilizes a temperature controlled water bath and a Vernier glass-body pH probe with Vernier Logger Pro 3.10.1 software for automated data collection. Data analysis is used to determine observed kinetic rate constants under the assumption that hydrolysis is a pseudo-first-order reaction. Eyring plots were used to compare activation energy parameters under iso-mole fraction conditions. The hydrolysis reaction of acetic anhydride was enthalpically stabilized and entropically destabilized at mole fractions of acetonitrile greater than 0.17 and the reverse occurred at mole fractions less than 0.17. Activation enthalpy and entropy result in the reaction being less favorable to form products as mole fraction of acetonitrile increased.

DEDICATION

This work is dedicated to my family: my parents, Larry and Kathy Mitchell; Sandy and Henry Stacy; my siblings, Jonathan Mitchell, Elizabeth Wallace, David Mitchell, Stephen Mitchell, and all their spouses; my nephew Jon Ed Mitchell, and to my colleagues at Virginia Highlands Community College, and to my friends who have supported me along my journey.

ACKNOWLEDGEMENTS

I would like to thank Dr. Dane Scott for being a great advisor. I would like to thank Samson Olowoyo for being a great friend and lab partner throughout the research for this work. I would also like to thank Dr. Greg Bishop and Dr. Marina Roginskaya for being on my thesis committee.

TABLE OF CONTENTS

	Page
ABSTRACT.....	2
DEDICATION.....	3
ACKNOWLEDGEMENTS.....	4
LIST OF TABLES.....	7
LIST OF FIGURES.....	8
LIST OF ABBREVIATIONS.....	9
Chapter	
1. INTRODUCTION.....	10
Kinetics of Acetic Anhydride Hydrolysis.....	10
Previously Used Kinetic Methods.....	11
The pH Technique for Kinetic Analysis.....	13
Acetonitrile and Its Effects on the Kinetics of Hydrolysis.....	14
Transition State Theory.....	15
Thermodynamic Analysis.....	16
Linear Solvent Energy Relationships.....	18
Research Objectives.....	20
2. METHODOLOGY.....	21
Materials Used.....	21
Preparation of Cosolvent Systems.....	21
Reaction Monitoring.....	22
3. RESULTS.....	25
Determination of Reaction Rate Constants.....	25
Iso-Mole Fraction Thermodynamic Analysis.....	26
Activation Entropy.....	29

Activation Enthalpy	29
Activation Gibbs Free Energy	30
LSER Analysis.....	32
4. DISCUSSION.....	34
Conclusion	36
Future Work	37
REFERENCES	38
VITA.....	41

LIST OF TABLES

Table	Page
1. Rate constants found via the pH technique.....	14
2. LSER parameters for water/acetonitrile cosolvent systems at 25°C	19
3. k_{obs} , min^{-1} , for acetic anhydride hydrolysis in water/acetonitrile cosolvent systems.....	25
4. Temperature-independent activation entropy and enthalpy determined by Eyring analysis under iso-mole fraction conditions.	28
5. Calculated activation Gibbs free energy for each temperature and mole fraction studied	28

LIST OF FIGURES

Figure	Page
1. Reaction mechanism for the hydrolysis of acetic anhydride	10
2. General reaction energy profile	16
3. Kamlet-Taft parameters vs. X_w at 25°C.....	19
4. Reaction vessel removed from circulator	23
5. Typical pH vs time plot for acetic anhydride hydrolysis in water/acetonitrile cosolvent $X_w=0.21$ at 30.0°C from pH probe 1 (orange) and pH probe 2 (blue).....	23
6. Example of data fit using equation (12). Coefficient d is k_{obs} . For this trial of $X_w=0.95$ at 30°C k_{obs} was found to be 0.1095 min ⁻¹ for pH probe 1 and 0.1128min ⁻¹ for pH probe 2	24
7. Isotherms for $-\log k_{obs}$ vs. X_w	26
8. Iso-mole fraction modified Eyring plots for acetic anhydride hydrolysis in water/acetonitrile cosolvent systems.....	27
9. Temperature-independent ΔS^\ddagger vs. X_w according to linear regression of equation 15	29
10. Temperature-independent ΔH^\ddagger vs. X_w according to linear regression of equation 15	30
11. Iso-mole fraction plot of ΔG^\ddagger vs. T in water/acetonitrile cosolvent systems. The lines from top to bottom represent X_w of 0.75, 0.79, 0.83, 0.87, 0.95, and 1.0	31
12. Isothermal ΔG^\ddagger vs. X_w for acetic anhydride hydrolysis in water/acetonitrile cosolvent systems. Lines from top to bottom represent 40°C, 30°C, 20°C, and 15°C	31
13. Isothermal $\log(k_x/k_w)$ vs. X_w , 15°C (blue), 20°C (orange), 30°C (grey), and 40°C (yellow) in water/acetonitrile cosolvent systems	32

LIST OF ABBREVIATIONS

ACN	Acetonitrile
E_a	Activation energy (also E_{act})
ΔG^\ddagger	Activation Gibbs free energy
ΔH^\ddagger	Activation enthalpy
h	Planck's constant
HBA	Hydrogen-bonding accepting parameter
HBD	Solvent hydrogen-bonding donating parameter
k'	Pseudo-first-order rate constant
k_B	The Boltzmann constant
k_{obs}	Observed rate constant
LSER	Linear Solvent Energy Relationships
MeCN	Acetonitrile
R	Ideal gas constant
ΔS^\ddagger	Activation entropy
TST	Transition State Theory

CHAPTER 1

INTRODUCTION

Kinetics of Acetic Anhydride Hydrolysis

Acetic anhydride, $(\text{CH}_3\text{CO})_2\text{O}$, is the simplest carboxylic anhydride and is commercially relevant in the synthesis of many different products including cellulose acetate, acetic acid, and aspirin.¹ The hydrolysis of acetic anhydride is a well-known reaction that has been studied in as early as 1906 and is known to occur in the irreversible three-step mechanism shown in Figure 1 with the addition of water being the rate-limiting step.² The transition state is denoted by the ‡ symbol.

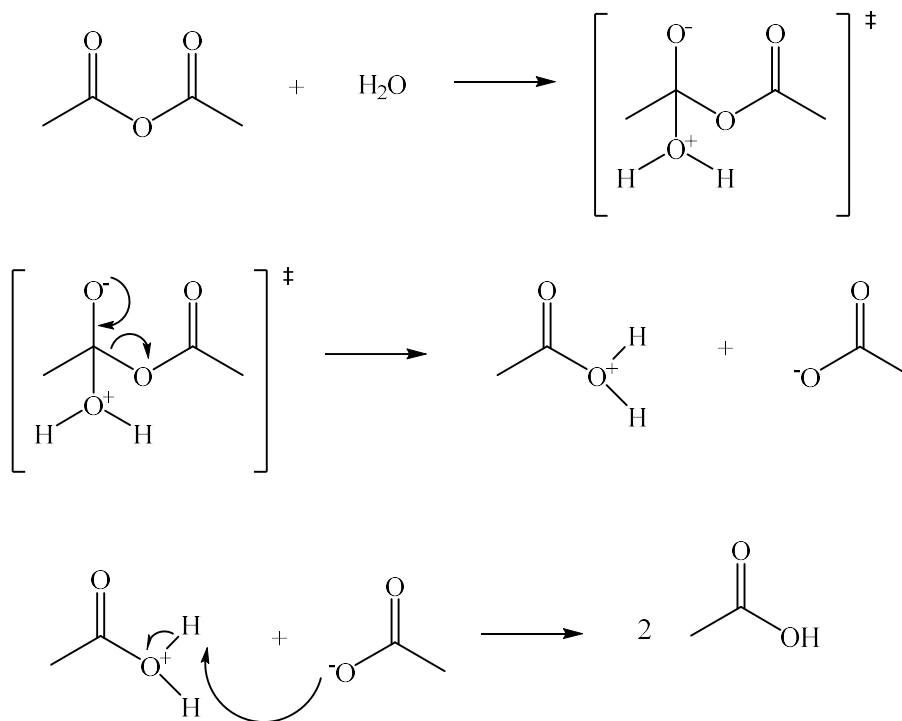


Figure 1: Reaction mechanism for the hydrolysis of acetic anhydride.²

With the addition step as the rate-limiting step of the mechanism, the reaction rate can be expressed as

$$-\frac{d(CH_3CO)_2O}{dt} = k[(CH_3CO)_2O][H_2O] \quad (1)$$

and is a true second-order reaction.² In most situations, the concentration of water is considerably higher than the concentration of acetic anhydride and the following pseudo-first-order rate law can be used in lieu of the more complex second order rate:

$$-\frac{d(CH_3CO)_2O}{dt} = k'[(CH_3CO)_2O] \quad (2)$$

The pseudo-first-order rate constant, k' , is the product of the second order rate constant, k , and the concentration of H_2O .

When acetic anhydride is at a much higher concentration than water, the rate constant changes as the reaction progresses. This occurs because the product of the hydrolysis, acetic acid, will catalyze the hydrolysis reaction.³ This auto-catalytic effect is negligible in experiments in which water is held at a much higher concentration than acetic anhydride but must be considered when the ratio is reversed.³

Previously Used Kinetic Methods

The methods used to study the kinetics of the hydrolysis reaction include but are not limited to: temperature-scanning², conductivity⁴, calorimetry⁵, and pH probing (which will be discussed in detail later in this chapter)⁶⁻⁷. Extensive literature on this reaction makes it ideal for the discovery of novel techniques that can be used in a wide spectrum of reactions to study kinetic parameters.⁶

The temperature scanning-technique is valuable as it results in an Arrhenius plot based on temperature vs. time data collected in near real-time.² This makes calculations of kinetic parameters more efficient since most historical measurements of kinetic parameters involved sample removal and analysis of the reaction system at predetermined time intervals.² Temperature scanning also offers advantage to previous isothermal measurements as it can collect data over a range of temperatures compared to single temperature allowing a large number of temperature-dependent kinetic parameters to be calculated in a single experiment.²

One form of calorimetric calculation of kinetic parameters involves collecting temperature vs. time data in non-adiabatic reaction vessels.⁵ The experimental setup is simple but the analysis is more complex than either of the two experimental setups outlined previously and involves determination of heat capacities for all equipment used in the experiment.^{2,4-5} Data collection is also simplified as this method only requires the initial concentration of acetic anhydride, initial concentration of water, and temperature change of the reaction including the temperature decrease after the reaction has gone to completion. The non-adiabatic method for determining kinetic parameters agrees with data at higher temperatures but fails at lower temperatures, potentially due to low solubility of acetic anhydride in water at low temperatures.⁵

Conductivity measurements can be used to monitor the kinetics of the hydrolysis reaction by continuously measuring the molar conductivity of the solution based on the production of acetic acid, which is a weak electrolyte.⁴ The conductivity also allows for the calculation of the extent of conversion of acetic anhydride to acetic acid. Conductivity measurements can be used to calculate the degree of conversion and therefore the kinetic parameters can be simultaneously compared to degree of conversions found by quenching the reaction with high a concentration of aniline which has a much faster reaction rate with acetic anhydride.^{2,4}

The pH Technique for Kinetic Analysis

A pH-based method to study kinetics in aqueous solution was developed to study the reaction kinetics of solvolytic decomposition of benzenediazonium tetrafluoroborate.⁷ In this method, pH vs. time data is collected and the data is fitted to the non-linear four-parameter equation shown below.⁶

$$pH = -\log \frac{\gamma K_{acid}}{2\gamma_+} - \log \left\{ 1 + \frac{4\gamma_+^2 [RCO_2H]_\infty}{\gamma K_{acid}} \left(1 - \frac{2[(RCO)_2O]_0 e^{-kt}}{[RCO_2H]_\infty} \right) - 1 \right\} \quad (3)$$

Where K_{acid} is the equilibrium constant for the acid reaction, γ is the activity coefficient for the undissociated acid, γ_+ is the activity coefficient of the hydronium ion, $[RCO_2H]_\infty$ is the concentration of the acid at reaction completion, and $[(RCO)_2O]_0$ is the initial concentration of the anhydride. The kinetic constants found using this method agree with the values found in literature and can be used for reactions that have a kinetic rate constant of less than 1 min^{-1} due to the response time of the pH electrode.⁶ The pH method has been shown to be effective and to agree with known values for the hydrolysis of acetic anhydride across a range of temperatures.⁶ Typical rate constants for the hydrolysis of acetic anhydride using the pH method are shown in Table 1 below. The value k'_W is the pseudo-first-order rate constant for the hydrolysis of acetic anhydride.

The pH technique is attractive as it requires inexpensive equipment and data can be fitted directly to the four-parameter equation easily using regression software.

Table 1: Rate constants found via the pH technique.⁶

t, °C	k'_w, min⁻¹	% of Standard Deviation
0.0	0.02582	1.9
2.5	0.03209	2.4
5.0	0.03848	1.7
7.5	0.04682	1.6
10.0	0.05481	1.1
12.5	0.06529	1.0
15.0	0.07768	0.82
20.0	0.1086	1.0
25.0	0.1479	0.40
30.0	0.1998	0.32
35.0	0.2624	0.52
40.0	0.3407	1.0
45.0	0.4423	0.48
50.0	0.5751	0.46
55.0	0.7427	0.69
60.0	0.9262	1.4
65.0	1.1640	0.92

Acetonitrile and Its Effect on the Kinetics of Hydrolysis

Acetonitrile (ACN) is an important cosolvent with water in organic synthesis, chromatography, hydrometallurgy, and other fields.⁸ Pure acetonitrile has been shown to exist in both monomeric and dimeric forms⁹, with multiple dimers including displaced antiparallel dimers and antiparallel cyclic dimers, which can trap low-energy electrons.¹⁰ For a binary system of water and acetonitrile, literature data show three separate regimes depending on the mole fraction of acetonitrile (X_{ACN}). One study used X-ray diffraction and ab-initio quantum mechanic calculations to study the structure of the water/acetonitrile cosolvent confirming the presence of microheterogeneous states at certain mole fractions of acetonitrile.¹¹ Another study by the same group used small-angle and large angle neutron diffraction paired with molecular dynamics simulations to determine that the maximum level of microheterogeneity occurs at

$X_{ACN}=0.38$. When X_{ACN} is less than 0.15, the tetrahedral voids in the water network are filled. If X_{ACN} is between 0.2 and 0.8, large clusters of ACN and water are formed resulting in microheterogeneous states. When X_{ACN} is greater than 0.8 water interferes with the bulk structure of acetonitrile.^{8,11}

The rate of acetic anhydride hydrolysis reactions depends on acetonitrile concentrations. In some cases, as the mole fraction of acetonitrile increases, the rate constant is lowered in other cases the rate constant increases with concentration of acetonitrile.^{12,13} One study on the reaction rate of 4-nitrophenyl chloroformate and 4-nitrophenyl heptafluorobutyrate using UV-Vis absorbance showed a minimum rate when the mole fraction of water (X_w) is 0.5.¹² Another study using UV-Vis absorbance for the hydrolysis reaction of p-nitrophenyl anthralite in water/acetonitrile cosolvent with X_w of 0.5 resulted in the lowest rate.¹³ These unexpected results are attributed to microheterogeneous states formed as the mole fraction of acetonitrile increases.

Transition State Theory

Transition state theory (TST) was developed in 1935 by Eyring and Polanyi and is based on the equilibrium between reactants and a transition state.¹⁴ For the reaction to occur, the reactant molecules must collide in such a manner as to have sufficient energy to overcome the reaction energy barrier between the reactant and the transition state.¹⁵ Energy vs. reaction coordinate is shown in Figure 2. The energy barrier between the reactant and transition state is the activation energy (E_{act}).

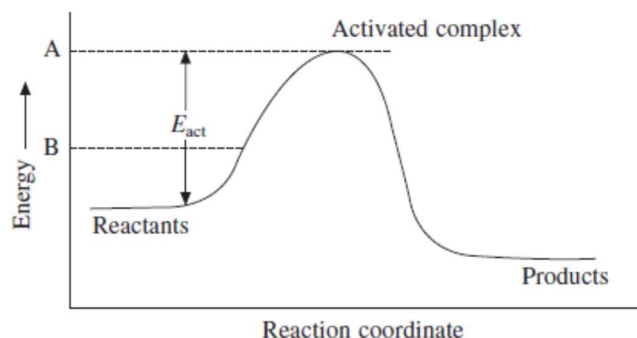


Figure 2: General reaction energy profile. E_{act} is activation energy and is the energy barrier between the reactants and the transition state or activated complex.¹⁴

The following equation shows the equilibrium between the reactants, transition state and formation of product.



In equation 4, the transition state, AB, is denoted by \ddagger , k_1 is the reaction rate constant for the forward equilibrium reaction, k_{-1} is the reaction rate constant for the reverse equilibrium reaction, and k_2 is the reaction rate constant for the second step.¹⁵ The reaction rate for equation 4 can be written as:

$$\frac{d[C]}{dt} = k_2 [AB^\ddagger] \quad (5)$$

Transition state theory is an important aspect of thermodynamic analysis.

Thermodynamic Analysis

Thermodynamic analysis is used to determine reaction parameters such as ΔH , ΔS , ΔG , and E_a among others. Methods for determining thermodynamic parameters are generally mathematical and include the Arrhenius equation, the van't Hoff equation, the Eyring equation, and many others.^{16,17,18} The three equations mentioned are shown in their linear forms below,

Arrhenius equation:

$$\ln(k) = \left(-\frac{E_a}{R}\right)\left(\frac{1}{T}\right) + \ln(A) \quad (6)$$

van't Hoff equation:

$$\ln(K_{eq}) = -\left(\frac{\Delta H}{R}\right)\left(\frac{1}{T}\right) + \frac{\Delta S}{R} \quad (7)$$

and Eyring equation:

$$\ln \frac{kh}{k_B T} = -\left(\frac{\Delta H^\ddagger}{R}\right)\left(\frac{1}{T}\right) + \frac{\Delta S^\ddagger}{R} \quad (8)$$

where k is the true reaction rate constant, K_{eq} is the equilibrium constant, E_a is activation energy, A is the pre-exponential factor, T is absolute temperature, R is the ideal gas constant, k_B is the Boltzmann constant, and h is Planck's constant. For the hydrolysis reaction of acetic anhydride, which proceeds as pseudo-first-order equation 8 is modified to:

$$\ln \frac{k_{obs}h}{k_B T [H_2O]} = -\left(\frac{\Delta H^\ddagger}{R}\right)\left(\frac{1}{T}\right) + \frac{\Delta S^\ddagger}{R} \quad (9)$$

since $k_{obs}=k[H_2O]$.¹⁸

The Arrhenius equation shows the dependence of the reaction rate constant on temperature and allows for the calculation of the activation energy for a given reaction. The van't Hoff equation relates the equilibrium constant to temperature to determine overall change in enthalpy and entropy. The modified Eyring equation, equation 9, was developed to determine activation parameters including activation entropy, activation enthalpy and activation Gibbs free energy for the hydrolysis of acetic anhydride.¹⁸ The modified Eyring equation required the temperature to be an independent variable and was used to study the reaction under iso-mole fraction and isodielectric conditions. This method used the above-mentioned four-parameter fit

of pH vs. time data to analyze a reaction for activation energy parameters.¹⁸ The novel method was compared to more conventional methods.

Linear Solvent Energy Relationships

Linear solvent energy relationships (LSER) relate solvent effects to two types of solute-solvent interactions: those involving hydrogen bonding complexing between solute and solvent and those that include changes in polarity/polarizability.¹⁹ LSER can be performed using a variety of different measurable properties, including free energy of formation, and can be used to determine the dependence of the chosen variable on solvent effects. The generalized form of LSER is given in equation (10):

$$P = P_0 + \text{cavity formation} + \text{dipolarity/polarizability} + \frac{HBD_{(1)}}{HBA_{(2)}} + \frac{HBA_{(1)}}{HBD_{(2)}} \quad (10)$$

where P is the measured property, P₀ is that property for a pure solvent, HBD is hydrogen bond donating parameter, HBA is the hydrogen-bond accepting parameter, and 1 and 2 refer to the solvent and solute, respectively.¹⁹ LSER has been modified to evaluate solvent effects on many different properties including free energy.¹⁸

The Kamlet-Taft linear solvent free energy relationship is given in equation (11) and can be used to determine the relationship between the solvent and the free energy of a reaction.

$$\log\left(\frac{k_x}{k_w}\right) = s\pi^* + a\alpha + b\beta \quad (11)$$

where k_x is the reaction rate constant at mole fraction of water in a cosolvent system, k_w is the reaction rate constant in pure water, π* is the polarity/polarization parameter, α is the solvent hydrogen bond donating parameter, β is the hydrogen-bond accepting parameter, and s, a, and b

are their respective solvatochromic coefficients.²⁰⁻²² The magnitude of the solvatochromic coefficients determine the contribution to the solvent effect.

LSER parameters have been determined for water/acetonitrile cosolvent systems over a range of X_w and are given in Table 2 below.²³ Figure 3 shows each parameter plotted against mole fraction of water.

Table 2: LSER parameters for water/acetonitrile cosolvent systems at 25°C.²³

X_w	π^*	α	β
1	1.14	1.13	0.58
0.9749	1.12	1.07	0.59
0.9535	1.1	1.03	0.59
0.9213	1.07	0.98	0.6
0.8723	1.03	0.94	0.61
0.6949	0.92	0.9	0.61

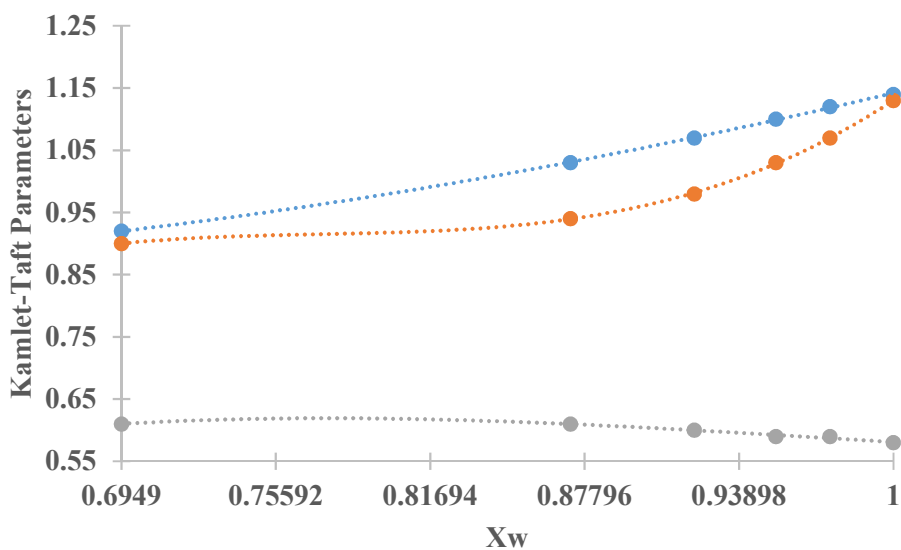


Figure 3: Kamlet-Taft parameters vs. X_w at 25°C. From top to bottom the lines represent π^* , α , and β .²¹

Research Objectives

The aim of this research is to determine the effect that ACN as a cosolvent has on activation energy in the hydrolysis of acetic anhydride. Since this reaction has been thoroughly studied, this reaction can be used with new methods for calibration purposes followed by similar studies of different reactions. Results will present reaction rate constants as well as activation energy parameters for aqueous hydrolysis of acetic anhydride in water/acetonitrile cosolvent solutions with X_{ACN} ranging from 0 to 0.25 and temperatures from 15.0 to 40.0°C.

CHAPTER 2

METHODOLOGY

Materials Used

Acetonitrile (General Use, $\geq 99.5\%$) used to make the cosolvent system was purchased from VWR International, LLC (Radnor, PA). Water used in cosolvent preparation was purified to $18.2\text{ M}\Omega$ using a Millipore Direct-Q[®] 3 UV with pump. Synthesis grade acetic anhydride ($\geq 98.0\%$) purchased from Merck KGaA (Darmstadt, Germany) was used as received in the simple hydrolysis reaction. Buffers of pH 4.00 (± 0.02) and 7.00 (± 0.02) used for calibration were purchased from Hach (Loveland, CO) and were used as received. Other miscellaneous materials included HCl, NaCl, and isopropyl alcohol.

Preparation of Cosolvent Systems

Water/acetonitrile cosolvent systems were prepared at mole fractions of 0.75, 0.79, 0.83, 0.87, 0.90, 0.92, 0.95, and 1, for water. All glassware was cleaned and rinsed using $18.2\text{ M}\Omega$ water and dried prior to use. Initially cosolvent systems were prepared in a 75 mL Erlenmeyer flask for single pH probes but were later prepared in a 100 mL three-neck round-bottom flask for two pH probes. The cosolvent systems were prepared by mass using an analytical balance and the amount of each cosolvent was calculated to give a pre-mixture volume of either 50 or 75 mL, and actual volumes were calculated later for each temperature and mole fraction. The reaction vessel was then submerged into a temperature-controlled water bath and magnetically stirred. Each cosolvent system was in the water bath for 10-15 min until the appropriate temperature was reached and the pH of the system stabilized. Acetic anhydride was dispensed using a

ThermoScientific FinnPipette F1 at a volume of either 125 μL for 50 mL of cosolvent or 188 μL for 75 mL of cosolvent.

Reaction Monitoring

The hydrolysis reaction was monitored by pH at each X_w at 15, 20, 30, and 40.00(± 0.01) $^{\circ}\text{C}$ controlled using a Fisher Scientific Isotemp 4100 R20. The temperature of the cosolvent system was checked using a mercury-in-glass thermometer. Plots consisting of pH vs. time were collected using one or two Vernier Glass-Body pH electrodes and analyzed using Vernier Logger Pro 3.10.1 software. The two-probe experimental setup is shown in Figure 4 below. The pH probes were calibrated using a two-point calibration at pH 4.01 and 7.00 before each trial. Data collection was started immediately upon addition of acetic anhydride and each trial lasted between 5 min and 30 hours during which 20 to 60 data points were collected. Four or more repeated trials were performed for each mole fraction at each temperature. Typical plots of pH vs. time for two pH probes used in tandem are shown in Figure 5. The two lines represent pH readings from each individual probe and differ due to the precision of the pH probes.

Regression analysis was performed using the following simplified form of equation (3)

$$pH = a - \log \left(\sqrt{(1 + b(1 - ce^{-dt}))} - 1 \right) \quad (12)$$

where a is $-\log \frac{\gamma K_{acid}}{2\gamma^+}$, b is $\frac{4\gamma_+^2 [RCO_2H]_{\infty}}{\gamma K_{acid}}$, c is $\frac{2[(RCO)_2]_0}{[RCO_2H]_{\infty}}$, and d is the pseudo-first-order rate constant k_{obs} . All trials were performed with pure cosolvent meaning that the γ values are constant. Figure 6 below shows an example set of data fit with equation (12) to determine k_{obs} .



Figure 4: Reaction vessel removed from circulator.

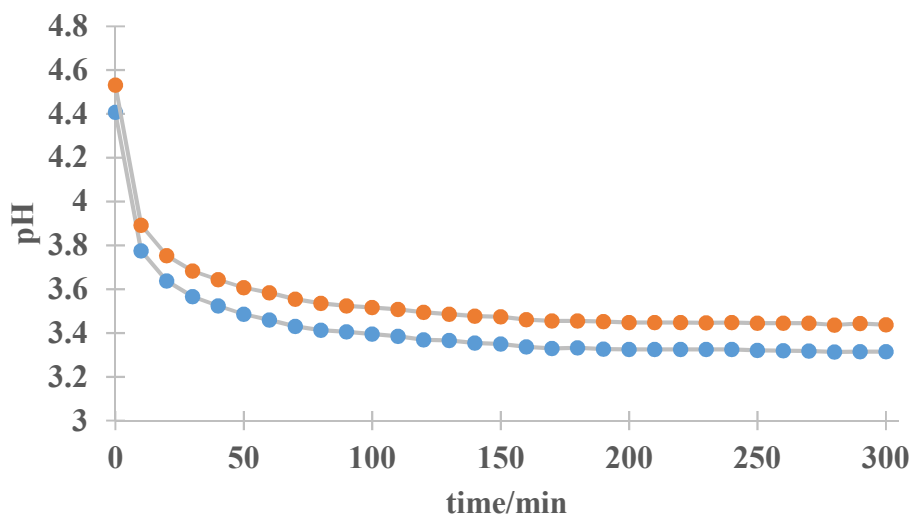


Figure 5: Typical pH vs time plot for acetic anhydride hydrolysis in water/acetonitrile cosolvent

$X_w=0.21$ at 30.0°C from pH probe 1 (orange) and pH probe 2 (blue).

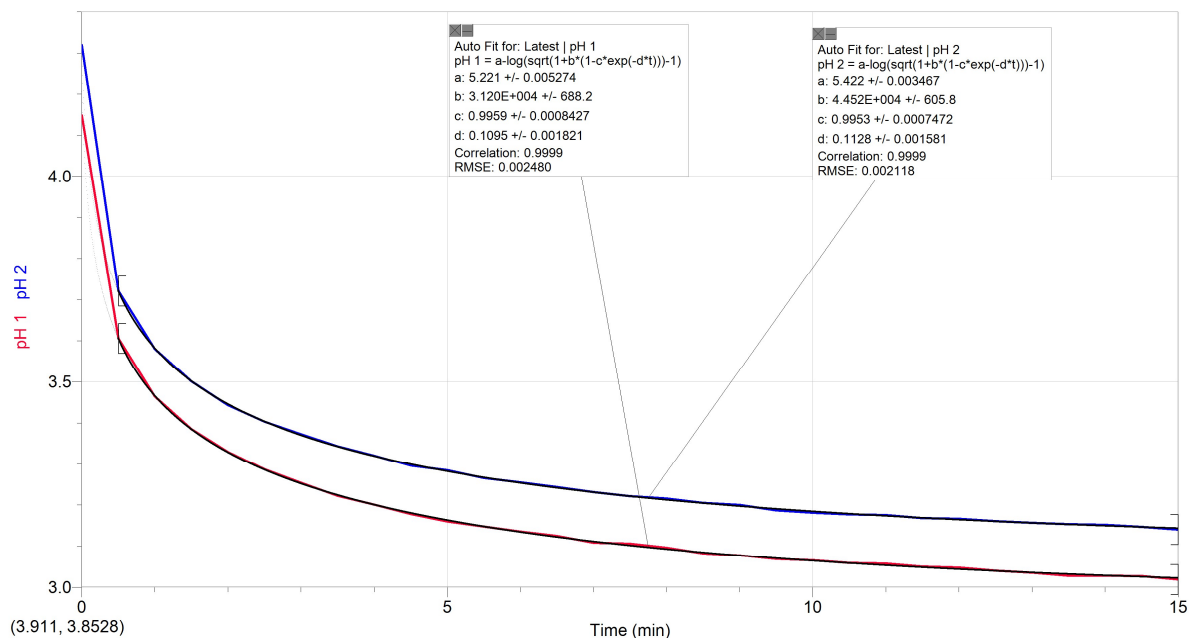


Figure 6: Example of data fit using equation (12). Coefficient d is k_{obs} . For this trial of $X_w=0.95$ at 30°C k_{obs} was found to be 0.1095 min^{-1} for pH probe 1 and 0.1128 min^{-1} for pH probe 2.

The collected pH vs. time data for each trial had a similar fit with correlation values of 0.97 or higher. All trials were fitted in as in Figure 6 where the first data point was not included in the regression. This is to avoid any undue influence from the dynamic region for this reaction as equation (3) requires the concentration of acetic acid at equilibrium and the initial concentration of acetic anhydride.

CHAPTER 3

RESULTS

Determination of Reaction Rate Constants

Graphs of pH vs. time data were analyzed using the four-parameter fit shown in equation (12) and k_{obs} was collected for X_w at each temperature. For each temperature, there was an increase in observed rate constant as X_w increased. The average rate constants are shown in Table 3.

Table 3: k_{obs} , min^{-1} for acetic anhydride hydrolysis in water/acetonitrile cosolvent systems.

X_w	k_{obs} , min^{-1} , for Various Mole Fractions and Temperatures			
	15.0°C	20.0°C	30.0°C	40.0°C
1	0.1101(±0.0037)	0.1406(±0.0065)	0.1687(±0.0130)	0.3035(±0.0124)
0.95	0.0505(±0.0044)	0.0477(±0.0028)	0.1097(±0.0038)	0.1145(±0.0046)
0.92	0.0215(±0.0008)	0.0296(±0.0023)	0.0623(±0.0032)	0.0757(±0.0017)
0.87	0.0158(±0.0003)	0.0253(±0.0000)	0.0302(±0.0023)	0.0408(±0.0006)
0.83	0.0100(±0.0011)	0.0109(±0.0021)	0.0191(±0.0003)	0.0214(±0.0031)
0.79	0.0058(±0.0003)	0.0071(±0.0007)	0.0124(±0.0006)	0.0156(±0.0008)
0.75	0.0034(±0.0001)	0.0048(±0.0003)	0.0079(±0.0003)	0.0096(±0.0005)

Constant temperature graphs (isotherms) of $-\log(k_{\text{obs}})$ vs X_w were plotted and shown in Figure 7.

If the $-\log(k_{\text{obs}})$ vs X_w is linear, $\left(\frac{\partial \Delta H^\ddagger}{\partial T}\right)_X$ and $\left(\frac{\partial \Delta S^\ddagger}{\partial T}\right)_X$ are equal to zero and therefore both

activation enthalpy and activation entropy are independent of temperature.

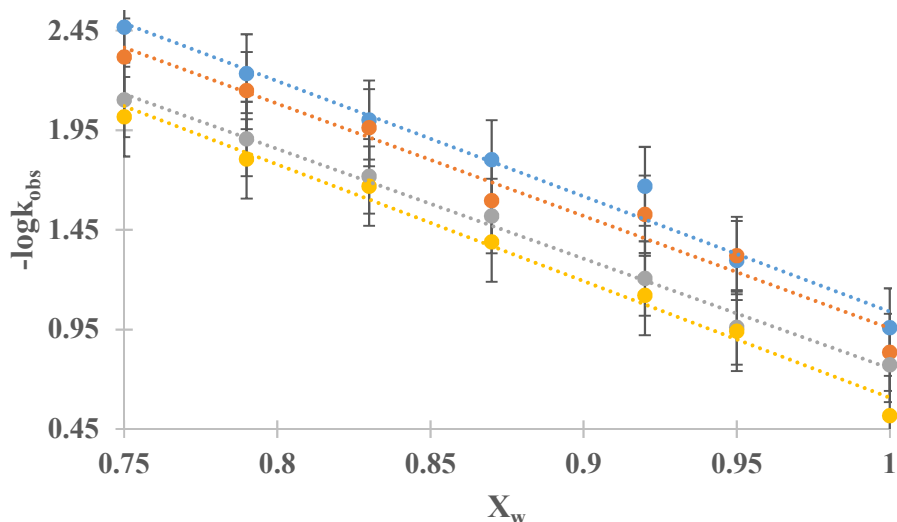


Figure 7: Isotherms for $-\log k_{\text{obs}}$ vs. X_w . Lines from top to bottom represent 15.0, 20.0, 30.0, and 40.0°C. Mole fractions of water from left to right are 0.75, 0.79, 0.83, 0.87, 0.92, 0.95, and exactly 1.

Iso-Mole Fraction Thermodynamic Analysis

The Eyring equation was chosen as a basis of thermodynamic analysis due to its reliability in aqueous phase reactions.¹⁸ Eyring analysis for the pseudo-first-order hydrolysis of acetic anhydride can be performed using equation 9. Further modifications to 9 simplify thermodynamic analysis. Multiplying both sides of equation 9 by the ideal gas constant gives equation 13.

$$R \left[\ln \frac{h k_{\text{obs}}}{k_B T} - \ln([H_2O]) \right] = \Delta S^\ddagger - \frac{\Delta H^\ddagger}{T} \quad (13)$$

Since all the terms on the left side of equation 13 are measured or constant values we can define the variable Y with units of $\text{J} \cdot \text{mol}^{-1} \cdot \text{K}^{-1}$ according to equation 14.

$$Y = R \left[\ln \frac{h k_{obs}}{k_B T} - \ln([H_2O]) \right] \quad (14)$$

Eyring analysis can then be performed via linear regression analysis using equation 15.¹⁸

$$Y = \Delta S^\ddagger - \frac{\Delta H^\ddagger}{T} \quad (15)$$

Iso-mole fraction Eyring plots are shown in Figure 8.

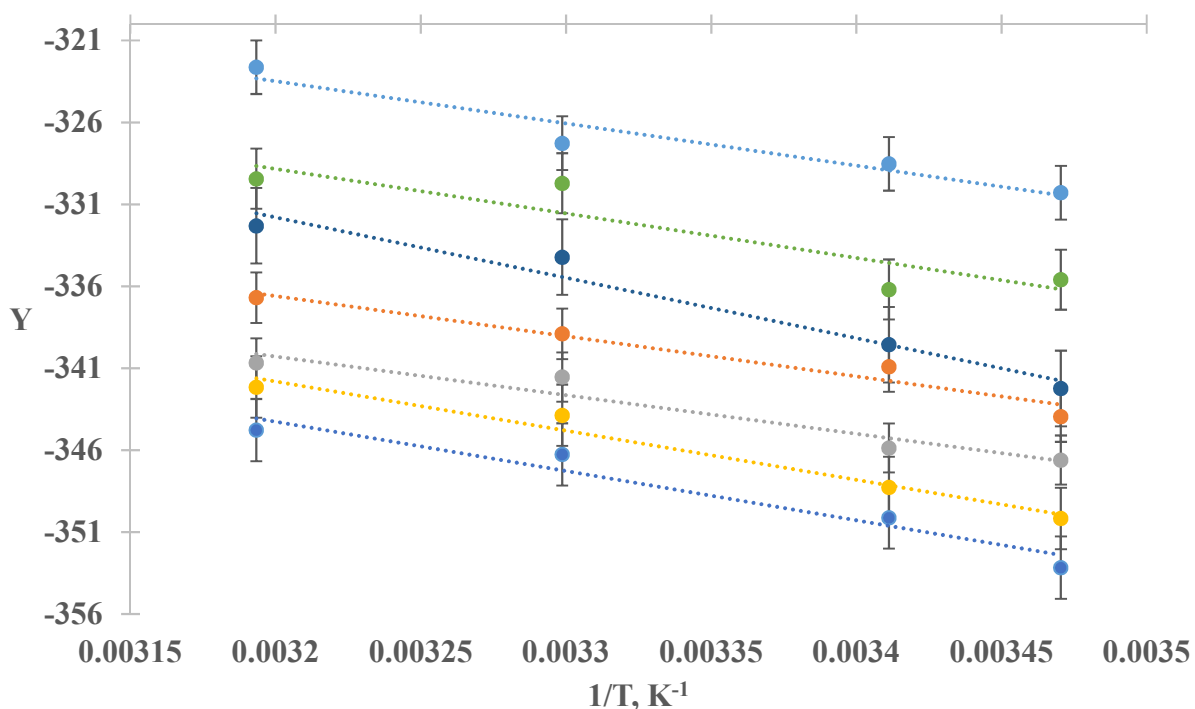


Figure 8: Iso-mole fraction modified Eyring plots for acetic anhydride hydrolysis in water/acetonitrile cosolvent systems. Lines from top to bottom represent X_w of 1.0, 0.95, 0.92, 0.87, 0.83, 0.79, and 0.75.

By plotting Y against inverse temperature at each mole fraction, activation entropy can be found using the y-intercept and activation enthalpy using the negative of the slope for the lines shown in Figure 8. Activation Gibbs free energy can be calculated using the relationship

$\Delta G^\ddagger = \Delta H^\ddagger - T(\Delta S^\ddagger)$.¹⁸ Activation enthalpy and entropy are given in Table 4 and calculated activation Gibbs free energies are in Table 5.

Table 4: Temperature-independent activation entropy and enthalpy determined by Eyring analysis under iso-mole fraction conditions.

X_w	$\Delta S^\ddagger, \text{J}\cdot\text{mol}^{-1}\cdot\text{K}^{-1}$	$\Delta H^\ddagger, \text{kJ}\cdot\text{mol}^{-1}$
1	-241.11(±16.46)	25.74(±4.92)
0.95	-254.80(±28.50)	23.13(±8.58)
0.92	-213.83(±16.74)	36.86(±5.00)
0.87	-258.21(±13.07)	24.50(±3.91)
0.83	-264.86(±14.96)	23.57(±4.47)
0.79	-245.81(±12.05)	30.00(±3.60)
0.75	-248.00(±16.89)	30.08(±5.05)

Table 5: Calculated activation Gibbs free energy for each temperature and mole fraction studied.

$\Delta G^\ddagger, \text{kJ}\cdot\text{mol}^{-1}$				
$t, ^\circ\text{C}$				
X_w	15.00	20.00	30.00	40.00
1	95.22(±4.92)	96.42(±4.92)	98.84(±4.92)	101.25(±4.92)
0.95	96.55(±8.58)	97.82(±8.58)	100.37(±8.58)	102.92(±8.58)
0.92	98.48(±5.00)	99.55(±5.00)	101.69(±5.00)	103.82(±5.00)
0.87	98.90(±3.91)	100.19(±3.91)	102.77(±3.91)	105.35(±3.91)
0.83	99.89(±4.47)	101.21(±4.47)	103.86(±4.47)	106.51(±4.47)
0.79	100.83(±3.60)	102.06(±3.60)	104.52(±3.60)	106.98(±3.60)
0.75	101.54(±5.05)	102.78(±5.05)	105.26(±5.05)	107.74(±5.05)

Activation Entropy

Isotherms for activation entropy between $X_w=0.75$ and $X_w=1.00$ for are plotted in Figure 9.

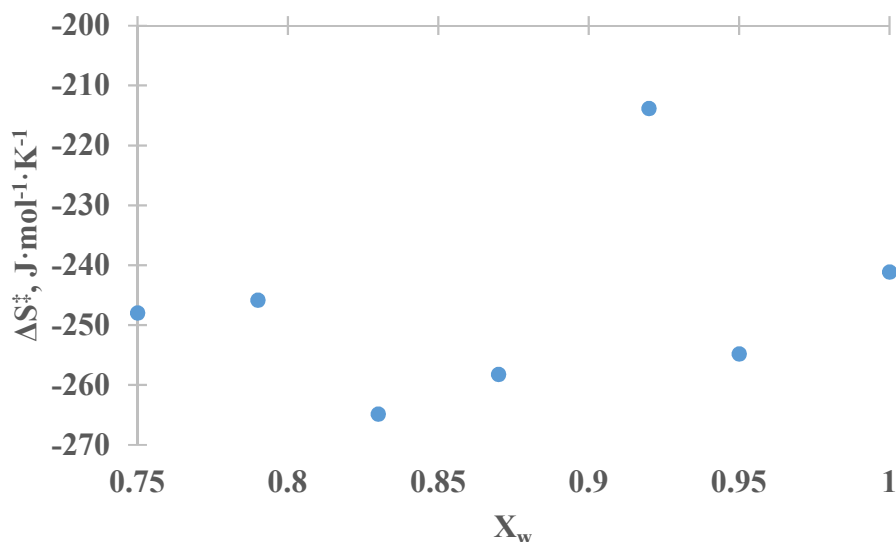


Figure 9: Temperature-independent ΔS^\ddagger vs. X_w according to linear regression of equation 15.

As can be seen in Figure 9 there is a decrease in activation entropy as X_w decreases from 1 to 0.83 followed by an increase in activation entropy as X_w decreases further to 0.75.

Activation Enthalpy

Calculated activation enthalpies showed similar trends as activation entropy. The activation enthalpy values showed the same trends based on compositional regimes as activation entropy (Figure 9).

Figure 10 shows the relationship of mole fraction and the stability of bulk water matrix. Converse to the nature of the relationship between ΔS^\ddagger and X_w in which the reaction was entropically destabilized in the $0.80 < X_w < 1$ region and stabilized in the $X_w < 0.8$ region, ΔH^\ddagger

shows the reaction is enthalpically stabilized in the $0.80 < X_w < 1$ and destabilized in the $X_w < 0.8$ region.

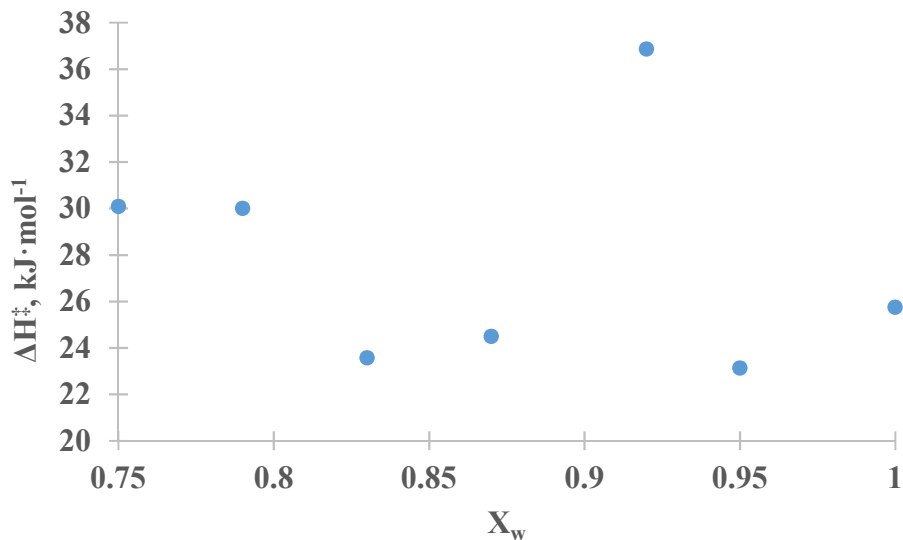


Figure 10: Temperature-independent ΔH^\ddagger vs. X_w according to linear regression of equation 15.

Activation Gibbs Free Energy

The activation Gibbs free energy showed linear relationships with both mole fraction and temperature. When iso-mole fraction ΔG^\ddagger were plotted against temperature there was a clear positive linear relationship for each mole fraction (Figure 11). The isothermal plot vs. mole fraction showed a clear negative linear relationship with increasing mole fraction (Figure 12). The slopes of both the isothermal and iso-mole fraction are similar across the various mole fractions and temperatures but have a standard deviation of nearly 10% in both cases.

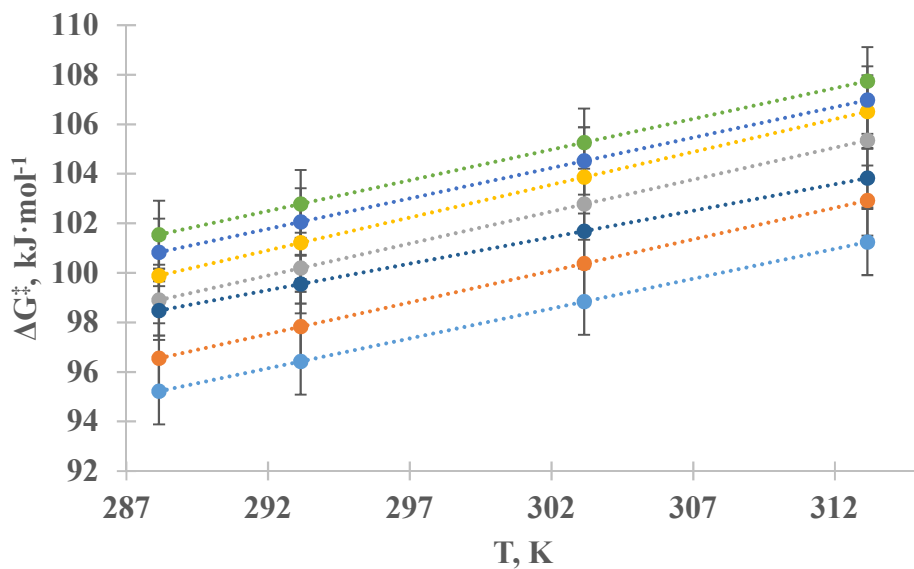


Figure 11: Iso-mole fraction plot of ΔG^\ddagger vs. T in water/acetonitrile cosolvent systems. The lines from top to bottom represent X_w of 0.75, 0.79, 0.83, 0.87, 0.95, and 1.0.

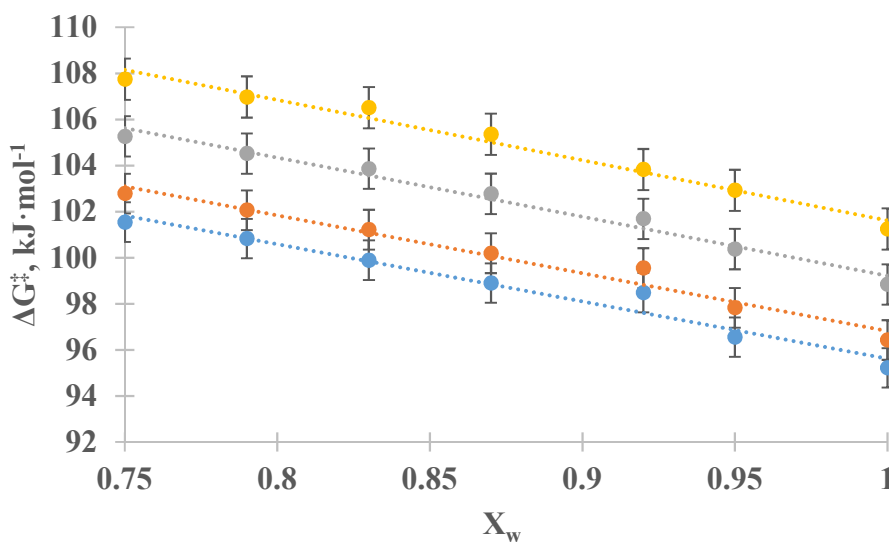


Figure 12: Isothermal ΔG^\ddagger vs. X_w for acetic anhydride hydrolysis in water/acetonitrile cosolvent systems. Lines from top to bottom represent 40°C, 30°C, 20°C, and 15°C.

LSER analysis

LSE analysis was performed using the Kamlet-Taft parameters listed in Table 3. $\log(k_x/k_w)$ was plotted against X_w and regression analysis was performed to determine the values of s , a , and b . The R^2 values were 0.9977. The plot of $\log(k_x/k_w)$ vs mole fraction for each temperature studied is shown in Figure 13. The average values of the solvatochromic coefficients for all four temperatures are $s = 7.24(\pm 0.63)$, $a = -1.75(\pm 0.28)$, and $b = -10.84(\pm 0.14)$.

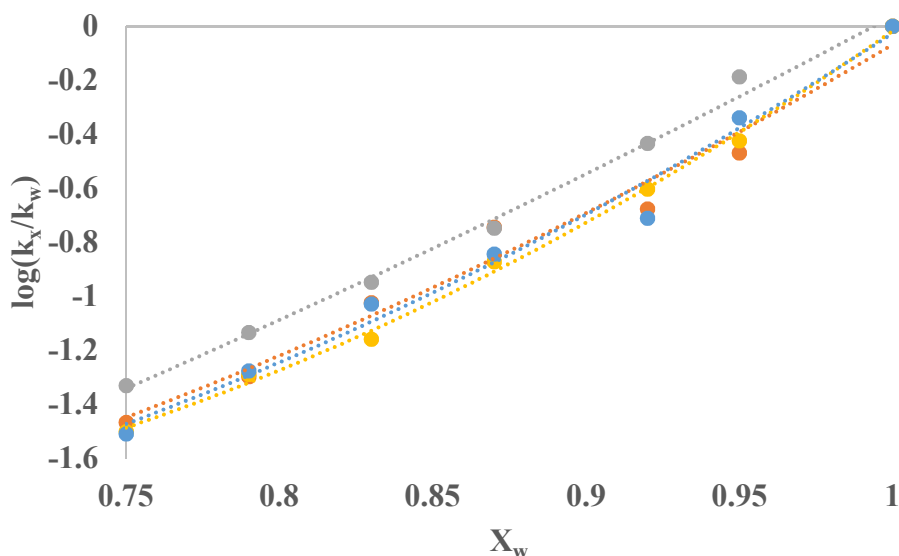


Figure 13: Isothermal $\log(k_x/k_w)$ vs. X_w , 15°C (blue), 20°C (orange), 30°C (grey), and 40°C (yellow) in water/acetonitrile cosolvent systems.

Differentiating equation (11) with respect to each solvatochromic parameter results in equations 17-19 which can be used to evaluate the effects of the cosolvent system on the acetic anhydride hydrolysis reaction.¹⁸

$$\left[\frac{\partial \log \left(\frac{k_x}{k_w} \right)}{\partial X_w} \right]_{\alpha, \beta} = s \left(\frac{d\pi^*}{dX_w} \right) \quad (17)$$

$$\left[\frac{\partial \log\left(\frac{k_x}{k_w}\right)}{\partial X_w} \right]_{\pi^*, \beta} = a \left(\frac{d\alpha}{dX_w} \right) \quad (18)$$

$$\left[\frac{\partial \log\left(\frac{k_x}{k_w}\right)}{\partial X_w} \right]_{\pi^*, \alpha} = b \left(\frac{d\beta}{dX_w} \right) \quad (19)$$

CHAPTER 4

DISCUSSION

The pseudo-first-order rate constants for acetic anhydride hydrolysis in water/acetonitrile cosolvent systems are lower than the values found in literature. The rate constants are within 20% of the values found by Wiseman et al. except rate constants found in pure water are statistically lower.¹⁸ The same mole fractions were studied across the temperature range to determine the effect of temperature on the rate of the hydrolysis of acetic anhydride. Direct comparisons are not possible as in previous work different mole fractions were used. As such, comparisons were made between the most similar mole fractions. The differences in the observed reaction constants may be due to differences in pH vs. time measurements. This work used an automated experimental set up while Wiseman et al. did not.¹⁸

The calculated values of ΔS^\ddagger , ΔH^\ddagger , and ΔG^\ddagger differ from those found in a recent article that performed the same analysis for the hydrolysis of acetic anhydride in water/acetonitrile cosolvent systems but the data in this work still follow a similar trend in which ΔS^\ddagger shows greater variation across mole fractions for a given temperature and ΔH^\ddagger shows considerably less variation.¹⁸ The ΔG^\ddagger values compare reasonably well between this work and the values found by Wiseman et al. and show the same trend of an increase in ΔG^\ddagger as mole fraction of water decreases and an increase in ΔG^\ddagger as temperature increases across the mole fraction range.¹⁸ The discrepancy with Wiseman et al. is likely due to differences in methods for determining Y—in this work the values were determined from experimental data for all points and in the earlier work many of the Y values were determined via polynomial regression rather than using equation 14.¹⁸

Literature shows three distinct relationships between acetonitrile mole fraction and stability of water. When X_{ACN} is less than 0.15, ACN will fill the voids in the water matrix, between X_{ACN} equal to 0.20 and X_{ACN} equal to 0.8 water and ACN form a stable complex, and when X_{ACN} is greater than 0.80 acetonitrile is the major solvent and water will fill the voids in the ACN matrix.^{8,11,19} Figure 9 shows an increase in activation entropy as X_w approaches 0.83 and a significant decrease at 0.87 followed by an increase toward that of water between 0.87 and 1.0.

The shape of the isothermal ΔH^\ddagger and ΔS^\ddagger graphs (Figures 9 and 10) appear to support the theory that water/acetonitrile cosolvent systems have distinct compositional regions. The values calculated for $X_{ACN}=0.08$ ($X_w=0.92$) do not agree with the trend seen for the other mole fractions for either ΔH^\ddagger or ΔS^\ddagger but the values for ΔG^\ddagger do follow the trends seen across the mole fraction range. The values for $X_{ACN}=0.08$ are believed to be anomalous and an explanation for this departure from the trend requires further work or analysis. The mole fraction range studied here does not focus on anything beyond X_{ACN} greater than 0.25 but there is a distinct change in both ΔH^\ddagger and ΔS^\ddagger between X_{ACN} of 0.17 and X_{ACN} of 0.21 (X_w of 0.83 and X_w of 0.79, respectively). The mole fraction range of $0.15 > X_{ACN} > 0.20$ is indicated in the literature to be the region where water-acetonitrile dimers begin to form and microheterogeneous states are present.^{8,11,19} More data would be needed to determine if the pH method of kinetic analysis would show the expected trend between $0.20 < X_{ACN} < 0.80$ in ΔH^\ddagger and ΔS^\ddagger .

The values found for the solvatochromic coefficients can be used with equations 17-19 to evaluate the effects of cosolvent systems on the stability of the reaction. Figure 3 shows that

$\left(\frac{d\pi^*}{dX_w}\right)$ is positive and s was found to also be positive so $\left[\frac{\partial \log\left(\frac{k_x}{k_w}\right)}{\partial X_w}\right]_{\alpha,\beta}$ is positive, indicating that as

X_w increases to 1 the role of solvent polarity/polarizability increases. The partial derivative $\left(\frac{d\alpha}{dX_w}\right)$ is positive above $X_w=0.85$ (Figure 3) and a was found to be negative so $\left[\frac{\partial \log\left(\frac{k_x}{k_w}\right)}{\partial X_w}\right]_{\pi^*,\beta}$ will be negative when $X_w>0.85$. Due to this it can be stated that the HBD parameter contributes to the stability of the reactant more than the transition state at $X_w>0.85$. The partial derivative $\left(\frac{d\beta}{dX_w}\right)$ is negative (Figure 2) and b was found to be negative making $\left[\frac{\partial \log\left(\frac{k_x}{k_w}\right)}{\partial X_w}\right]_{\pi^*,\alpha}$ positive. Since $\left[\frac{\partial \log\left(\frac{k_x}{k_w}\right)}{\partial X_w}\right]_{\pi^*,\alpha}$ is positive, the contribution of HBA decreases as X_w increases and that the reactant is stabilized more than the transition state which is supported by values found for ΔG^\ddagger .

Conclusion

The pH technique for kinetic analysis is appealing as reaction monitoring has been automated and instrumentation is inexpensive compared to other techniques. Values for pseudo-first-order rate constants for hydrolysis of acetic anhydride have determined in water/acetonitrile cosolvents for mole fractions of water between $X_w=0.75$ and $X_w=1.0$ for 15.00, 20.00, 30.00 and 40.00° C. For each temperature studied, the observed reaction rate constant decreased with decreasing mole fraction of water. An increase in reaction rate constant was seen for each mole fraction as temperature increased. These trends are in agreement with literature values for acetic anhydride hydrolysis.¹⁸

Iso-mole fraction Eyring analysis was used to determine activation entropy and activation enthalpy which were then used to calculate activation Gibbs free energy. The activation entropy and activation enthalpy were found to be independent of temperature. The activation Gibbs free

energy analysis showed that formation of the transition state and therefore the reaction overall becomes less favorable as mole fraction of water decreases isothermally and as temperature increases under iso-mole fraction conditions. Activation entropy and activation enthalpy shows more complex relationships with the stability of the reaction. Entropic destabilization and enthalpic stabilization of the transition state occur as mole fraction of water decreases to 0.8 and reverse as mole fraction further decreases to 0.75. These trends agree with the Kamlet-Taft LSER analysis. The values for activation entropy and activation enthalpy as well as the LSER analysis are attributed to the development of microheterogeneous states in water/acetonitrile cosolvent systems but further studies are needed.

Currently the pH technique for kinetic analysis is novel and disagreements in reported values may be due to several possible factors: raw data collection technique, calculation methods used for Eyring analysis and other experimental variables such as stirring. Even though the calculated values differed from literature values for the activation energy parameters, the trends obtained are in agreement with literature.¹⁸ Development of a generalized experimental design for the pH technique of kinetic analysis of hydrolysis reactions is needed and further refinement of the technique may lead to a better agreement with literature values.

Future Work

Studies performing kinetic analysis using the pH technique on larger values of X_{ACN} should be explored to determine if the activation energy parameters follow the compositional regimes for water/acetonitrile cosolvent systems. The methodology outlined in this work can also be adapted to study the hydrolysis of acetic anhydride in many cosolvent systems and future work is already planned. Replication studies are needed for the pH method of kinetic analysis to determine if it is a valuable and accurate tool for thermodynamic analysis.

REFERENCES

1. Gómez García, M. Á.; Dobrosz-Gómez, I.; Ojeda Toro, J. C., Thermal stability and dynamic analysis of the acetic anhydride hydrolysis reaction. *Chem. Eng. Sci.* **2016**, 142, 269-276.
2. Asprey, S. P.; Wojciechowski, B. W.; Rice, N. M.; Dorcas, A., Applications of temperature scanning in kinetic investigations: The hydrolysis of acetic anhydride. *Chem. Eng. Sci.* **1996**, 51, 4681-4692.
3. Fritzler, B. C.; Dharmavaram, S.; Hartrim, R. T.; Diffendall, G. F., Acetic Anhydride Hydrolysis at High Acetic Anhydride to Water Ratios. *Int. J. Chem. Kinet.* **2014**, 46, 151-160.
4. Kralj, A. K., Checking the kinetics of acetic acid production by measuring the conductivity. *J. Ind. Eng. Chem.* **2007**, 13, 631-636.
5. Hirota, W. H.; Rodrigues, R. B.; Sayer, C.; Giudici, R., Hydrolysis of acetic anhydride: Non-adiabatic calorimetric determination of kinetics and heat exchange. *Chem. Eng. Sci.* **2010**, 65, 3849-3858.
6. Wiseman, F. L., New insight on an old reaction - the aqueous hydrolysis of acetic anhydride. *J. Phys. Org. Chem.* **2012**, 25, 1105-1111.
7. Wiseman, F. L., Monitoring the Rate of Solvolytic Decomposition of Benzenediazonium Tetrafluoroborate in Aqueous Media Using a pH Electrode. *J. Chem. Educ.* **2005**, 82, 1841.
8. Bakó, I.; Megyes, T.; Grósz, T.; Pálinkás, G.; Dore, J., Structural investigation of water-acetonitrile mixtures: Small-angle and wide-angle neutron diffraction study compared to molecular dynamics simulation. *J. Mol. Liq.* **2006**, 125, 174-180.

9. Brakaspathy, R.; Singh, S., Geometry optimization of acetonitrile monomer and dimers using CNDO/force method. *J. Chem. Sci.* **1986**, 96, 285.
10. Timerghazin, Q. K.; Peslherbe, G. H., Electronic Structure of the Acetonitrile and Acetonitrile Dimer Anions: A Topological Investigation. *J. Phys. Chem. B* **2008**, 112, 520-528.
11. Bakó, I.; Megyes, T.; Pálinkás, G., Structural investigation of water–acetonitrile mixtures: An ab initio, molecular dynamics and X-ray diffraction study. *Chem. Phys.* **2005**, 316, 235-244.
12. El Seoud, O. A.; Siviero, F., Kinetics of the pH-independent hydrolyses of 4-nitrophenyl chloroformate and 4-nitrophenyl heptafluorobutyrate in water-acetonitrile mixtures: consequences of solvent composition and ester hydrophobicity. *J. Phys. Org. Chem.* **2006**, 19, 793-802.
13. Bayissa, L. D.; Ohmae, Y.; Hojo, M., Specific influence of salts on the hydrolysis reaction rate of p-nitrophenyl anthranilate in binary acetonitrile–water solvents. *J. Mol. Liq.* **2014**, 199, 294-300.
14. Upadhyay, S.K. *Chemical Kinetics and Reaction Dynamics*; Springer: New York, 2006; pp. 79-92.
15. Houston, P. L. *Chemical Kinetics and Reaction Dynamics*; Dover Publications: Mineola, NY, 2006. pp. 102-109.
16. Haghani, A.; Saeva, D. R.; Iloukhani, H.; Hoffmann, M. M., Comparing Composition- and Temperature-Dependent Viscosities of Binary Systems Involving Ionic Liquids. *J. Chem. Eng. Dat.* **2015**, 60, 3272-3288.

17. Horn, J. R.; Brandts, J. F.; Murphy, K. P., van't Hoff and Calorimetric Enthalpies II: Effects of Linked Equilibria. *Biochemistry* **2002**, 41, 7501-7507.
18. Wiseman, F. L.; Scott, D. W.; Cooper, W. C.; Tamine, J.; O'Connell, R.; Mitchell, N., Detailed thermodynamic analysis of the activation parameters for the simple hydrolysis of acetic anhydride in the acetonitrile/water cosolvent system. *RSC Advances* **2017**, 7, 28965-28978.
19. W. Taft, R.; Abboud, J.-L.; J. Kamlet, M.; H. Abraham, M., Linear Solvation Energy Relations. *J. Solution. Chem.* **1985**; Vol. 14, p 153-186.
20. Kamlet, M. J.; Abboud, J. L.; Taft, R. W., The solvatochromic comparison method. 6. The π^* scale of solvent polarities. *J. Am. Chem. Soc.* **1977**, 99, 6027-6038.
21. Taft, R. W.; Kamlet, M. J., The solvatochromic comparison method. 2. The alpha-scale of solvent hydrogen-bond donor (HBD) acidities. *J. Am. Chem. Soc.* **1976**, 98, 2886-2894.
22. Kamlet, M. J.; Taft, R. W., The solvatochromic comparison method. I. The beta-scale of solvent hydrogen-bond acceptor (HBA) basicities. *J. Am. Chem. Soc.* **1976**, 98, 377-383.
23. Barbosa, J.; Hernández-Cassou, S.; Sanz-Nebot, V.; Toro, I., Variation of acidity constants of peptides in acetonitrile-water mixtures with solvent composition: effect of preferential solvation. *J. Pept. Res.* **1997**, 50, 14-24.

VITA

NATHAN MITCHELL

- Education: M.S. East Tennessee State University, Johnson City, TN (May 2018)
B.S. Emory & Henry College, Emory, VA (July 2013)
- Employment: Tutor, Virginia Highlands Community College, Abingdon, VA (January 2010 – May 2018)
- Teaching: Adjunct Instructor, Virginia Highlands Community College (September 2013 – May 2018)
Teaching Assistant, East Tennessee State University (August 2017 – May 2018)
- Publications: Wiseman, F. L.; Scott, D. W.; Cooper, W. C.; Tamine, J.; O'Connell, R.; Mitchell, N., Detailed thermodynamic analysis of the activation parameters for the simple hydrolysis of acetic anhydride in the acetonitrile/water cosolvent system. *RSC Advances* 2017, 7, 28965-28978.
- Presentations: Nathan Mitchell, Samson Olowoyo, Dane W. Scott, and Floyd Wiseman. Eyring Activation Energy Analysis of Acetic Anhydride Hydrolysis in Cosolvent Systems, 69th South East Regional Meeting of the American Chemical Society, Charlotte, NC., 2017, (11/9/2017, Poster Presentation, SERMACS 2017)
Nathan Mitchell. Eyring Activation Energy Analysis of Acetic Anhydride Hydrolysis in Acetonitrile Cosolvent Systems, (3/16/18) Graduate Seminar, ETSU